The Journal of Neuroscience, September 1995, 15(9): 6110–6123

Inactivating and Noninactivating Ca^{2+}- and Voltage-Dependent K^+ Current in Rat Adrenal Chromaffin Cells

C. R. Solaro, M. Prakriya, J. P. Ding, and C. J. Lingle

Washington University School of Medicine, Department of Anesthesiology, St. Louis, Missouri 63110

The properties of Ca^{2+}- and voltage-dependent K^+ currents and their role in defining membrane potential were studied in cultured rat chromaffin cells. Two variants of large-conductance, Ca^{2+} and voltage-dependent BK channels, one noninactivating and one inactivating, were largely segregated among patches. Whole-cell noninactivating and inactivating currents resulting from each of these channels were segregated among different chromaffin cells. Cell-to-cell variation in the rate and extent of whole-cell current decay was not explained by differences in cytosolic $[Ca^{2+}]$ regulation among cells; rather, variation was due to differences in the intrinsic properties of the underlying BK channels. About 75% of rat chromaffin cells and patches express inactivating BK current (termed BK_i) while the remainder express noninactivating BK current (termed BK_s). The activation time course of both currents is similar, as is the dependence of activation on $[Ca^{2+}]$ and membrane potential. However, deactivation of BK_i channels is slower than that of BK_s channels.

The functional role of these BK channel variants was studied in current-clamp recordings. Although both BK_i and BK_s currents contribute to action potential repolarization, cells expressing BK_i current are better able to fire repetitively in response to constant current injection. Blockade of BK_i current by charybdotoxin abolishes this behavior, showing that afterhyperpolarizations mediated by BK_i current are permissive for repetitive firing. Thus, important properties of chromaffin cell membrane excitability are determined by the type of BK current expressed.

[Key words: BK channels, inactivation, chromaffin cells, Ca^{2+}-dependent K^+ currents, afterhyperpolarizations, catecholamine secretion, K^+ channel inactivation]

Rat adrenal chromaffin cells express two kinds of calcium-activated potassium current (Neely and Lingle, 1992a). One current, termed BK current, results from a large-conductance, voltage- and calcium-dependent channel that is blocked by tetraethylammonium (TEA) ions (Marty, 1981; Marty and Neher, 1985; Neely and Lingle, 1992a). The second current, termed SK current, is voltage independent and is blocked by apamin and curare (Neely and Lingle, 1992a; Park, 1994). Unlike BK current described in most other cell types, BK current in the majority of rat chromaffin cells exhibits rapid and complete inactivation (Solaro and Lingle, 1992; Herrington et al., 1995). Inactivation of whole-cell BK current results from the intrinsic inactivation of single BK channels, which we have studied in excised patches both from rat chromaffin cells and PC12 cells (Solaro and Lingle, 1992). We have also shown that noninactivating BK channels can be observed in patches from some cells. The presence of inactivating and noninactivating BK channels in separate membrane patches raises the possibility that chromaffin cells can differentially express different types of BK channels.

BK channels in most mammalian cells exhibit sustained activity in the presence of a fixed voltage and cytoplasmic calcium concentration ($[Ca^{2+}]_i$). In addition, they undergo rapid activation and deactivation following changes in membrane potential (Adams et al., 1982; Neely and Lingle, 1992a). Therefore, these channels are thought to sense rapid changes in both membrane voltage and $[Ca^{2+}]_i$ and have been proposed to play a role in fast action potential repolarization (Adams et al., 1982; Lancaster and Adams, 1986; Lancaster and Nicoll, 1987; Lancaster and Pennefather, 1987; Lang and Ritchie, 1987, 1990). Inactivating and noninactivating members of the voltage-gated K^+ channel family are thought, in general, to underly distinct physiological processes (Hille, 1992). By analogy, inactivating BK current in rat chromaffin cells might be expected to play a physiological role different than that of noninactivating BK current.

Here, we show that inactivating and noninactivating BK channels are segregated among distinct chromaffin cells. We describe the relative occurrence of inactivating and noninactivating BK channels among rat chromaffin cells and PC12 cells and compare some of the properties of these two natural BK channel variants. We show that the differences in the time course of BK current following robust elevations of cytosolic $[Ca^{2+}]_i$ result not from differences in the time course of $[Ca^{2+}]_i$ changes, but from the intrinsic properties of the BK channels themselves. Furthermore, whether cytosolic $[Ca^{2+}]$ is elevated by depolarization-elicited influx, muscarine-induced release from cytosolic Ca^{2+} stores, or via direct introduction of Ca^{2+} from a recording pipette, a similar diversity in BK current behavior is observed. Current-clamp experiments demonstrate that the ability of chromaffin cells to repetitively fire action potentials depends critically on the type of BK current present. Expression of a specific BK channel variant may permit particular action potential firing patterns in response to sustained depolarizing stimuli. These patterns may, in turn, influence the temporal properties of secretion stimulated by particular secretagogues.

Materials and Methods

Chromaffin cell culture. Methods of rat chromaffin cell isolation and maintenance of cultures were as described in Neely and Lingle (1992a)

Received Mar. 15, 1995; revised May 11, 1995; accepted May 12, 1995.

This work was supported by DK-46564 from the National Institutes of Health. We thank J. Nerbonne for review of the manuscript.

Correspondence should be addressed to C. Lingle at the above address.

and Herrington et al. (1995), and were based on procedures described in several earlier studies (Fenwick et al., 1978; Kilpatrick et al., 1980; Role and Perlman, 1980; Livett, 1984). Each chromaffin cell dispersion was typically done on adrenal medullas from three to four rats of about 2–3 months age.

Culture of PC12 cells. PC12h cells (Hatanaka, 1981) were maintained in gelatinized 50 ml tissue culture flasks containing 10 ml of plating media [Dulbecco's Modified Eagle's medium (DMEM), 10% fetal bovine serum (FBS), and 5% horse serum (HS)]. Flasks were stored in a humidified incubator at 37°C with 5% CO_2. Cells were passaged weekly by gently washing cells from the flask wall into a 15 ml plastic centrifuge tube, and triturating with a Pasteur pipette until cell clumps were broken into mostly single cells. Cells were counted using a hemacytometer, and plating media was added to obtain a density of 10^4 cells per ml. Ten milliliters of this suspension were added to new tissue culture flasks, which were then placed back into the incubator. Cells left over from passaging were plated onto collagen-coated (Vitrogen, Celltrix Labs) 35 mm tissue culture dishes (Corning) and incubated. For some experiments, nerve growth factor (100 ng/ml) or dexamethasone (1 μM) was added to the cell suspension just before plating. Currents were recorded from PC12 cells 1–7 d after plating.

Electrophysiological methods. Whole-cell and single-channel currents were recorded 2–14 d after chromaffin cells were plated. Most whole-cell currents were recorded using the perforated patch method (Horn and Marty, 1988), with amphotericin as the permeabilizing agent (Rae et al., 1991). For experiments in which a solution of defined $[Ca^{2+}]_i$ was introduced into cells, the standard whole-cell recording procedure was used (Hamill et al., 1981). Whole-cell currents were recorded with an Axopatch 1-A amplifier (Axon Instruments, Foster City, CA) using a 500 MΩ feedback resistor. Single-channel currents were recorded with an Axopatch 1C amplifier (Axon Instruments) using a 50 GΩ feedback resistor. For current-clamp experiments, the perforated-patch method was used with an Axoclamp 2A amplifier (Axon Instruments) in single-electrode discontinuous mode.

In perforated patch experiments, uncompensated series resistance (R_s) was typically 5–20 MΩ of which 80–95% was electronically compensated. In most cases, residual uncompensated R_s was less than 2 MΩ which, for currents up to 5 nA, results in at most a 10 mV error in the effective command potential. Larger errors (10–20 mV) were considered tolerable in experiments when an accurate measurement of current time course was not critical. Values for R_s and the percentage compensation for specific experiments are provided in the figure legends. Cell voltages during whole-cell recordings were controlled with the Clampex program from the pCLAMP software package (Axon Instruments, Foster City, CA). Similarly, Clampex was used to generate repetitive voltage pulse sequences to activate BK channels in single-channel recordings. Analysis of whole-cell and single-channel currents was done with our own software.

Data analysis. Currents or extracted data were fitted using a Levenberg-Marquardt search algorithm to obtain nonlinear least-squares estimates of function parameters. Kinetic properties of whole-cell and ensemble average currents were described by fitting currents with a Hodgkin-Huxley model of inactivating current (Hodgkin and Huxley, 1952):

$$I(t) = I_{max} * m(t)^n * h(t) \quad (1)$$

with

$$m(t) = 1 - \exp(-t/t_m),$$
$$h(t) = h_{inf} - (h_{inf} - 1.0) * \exp(-t/\tau_h), \quad (2)$$

where I_{max} is the maximal activatable outward current, τ_m is the activation time constant, n is the cooperativity in the activation process, τ_h is the inactivation time constant, and h_{inf} is the fraction of residual noninactivating current. In most experiments, 100 or 200 nM apamin was added to the external saline to minimize the contribution of SK current to the Ca^{2+}-dependent current.

Solutions. The usual extracellular solution contained the following (in mM): 140 NaCl; 5.4 KCl; 10 [N-(2-Hydroxyethyl)piperazine-N'-(2-ethanesulfonic acid)] (HEPES); 1.8 $CaCl_2$, and 2.0 $MgCl_2$, pH 7.4, adjusted with N-methylglucamine (NMG). For perforated patch experiments, the pipette saline contained the following (in mM): 120 K-aspartate, 30 KCl, 10 HEPES(H^+), 2 $MgCl_2$ adjusted to pH 7.4 with NMG. Membrane permeabilization was accomplished with a mixture of amphotericin B (Rae et al., 1991) and pluronic acid as described previously (Herrington et al., 1995). Osmolarity was measured by dew point (Wescor Osmometer) and adjusted within 3% (internal saline, 290; external saline: 305). Tetraethylammonium ion (TEA), charybdotoxin (CTX), iberiotoxin (IBX), and apamin were each added directly to the extracellular saline without additional adjustments.

For single-channel recordings, cells were bathed in the extracellular saline used for whole-cell recordings described above. Just prior to patch excision, the solution bathing the cell was changed to the 0 Ca^{2+} saline described below. For inside-out single-channel recordings, the pipette saline contained (in mM) 140 KCl, 20 KOH, 2 $MgCl_2$, 10 HEPES, pH 7.0, adjusted with 1 N HCl. The cytosolic saline used during excised inside-out patch recordings was the following (in mM): 140 KCl, 20 KOH, 10 HEPES, 5 Ethylene glycol-bis(β-aminoethyl ether) N,N,N',N'-tetraacetic acid (EGTA) with added $CaCl_2$ to make the desired free $[Ca^{2+}]$, pH 7.0, adjusted with 1 N HCl. N-Hydroxyethylethylene-diaminetriacetic acid (HEDTA) was used to buffer Ca^{2+} in solutions with desired free $[Ca^{2+}]$ greater than 2 μM. Estimates of free $[Ca^{2+}]$ were determined as described previously (Solaro and Lingle, 1992; Herrington et al., 1995).

Voltages for perforated-patch whole-cell recordings have been corrected for a +9 mV liquid junction potential, which results from the use of a K-aspartate–based pipette saline. A correction was also made for the +3 mV liquid junction potential that arose when chloride-based salines were used for introducing high $[Ca^{2+}]$ into cells.

Solution exchange and drug applications were accomplished as described previously (Herrington et al., 1995). Pluronic acid was from Molecular Probes, Eugene, OR. All other chemicals were from Aldrich or Sigma. Charybdotoxin (CTX) and recombinant iberiotoxin (IBX) were the generous gifts of our colleagues at the Merck Research Labs. CTX, obtained from Peninsula Labs, was used in some experiments. Nerve growth factor (NGF) was the kind gift of Dr. Eugene M. Johnson (Washington University, St. Louis).

Results

Selective expression of single BK_s and BK_i channels in rat chromaffin cells

Single-channel recordings from excised inside-out patches of rat chromaffin cells reveal two distinct types of BK channels (Fig. 1). Both channel types have a similar single-channel conductance (~270 pS in symmetrical K^+). Activation of both types requires $[Ca^{2+}]_i$ and membrane depolarization, but one form inactivates within 35–50 msec at 2 μM Ca^{2+}_i or higher (Solaro and Lingle, 1992). A tabulation of the frequency of observation of each channel type shows that the two types appear to be differentially segregated among patches (Table 1). In particular, of 446 patches, 338 (75.8%) contained exclusively inactivating BK channels, 41 (9.2%) contained exclusively noninactivating BK channels, and the remaining 15% contained both types of channel. Since patches with inactivating channels usually contained 3–10 channels, these distributions are unlikely to result from the random expression of two BK channel variants on all chromaffin cells. These data suggest two possibilities: each type of BK channel occurs in clusters, or a particular chromaffin cell expresses one type preferentially. Recordings of whole-cell BK current shown below support the latter possibility. We will refer to inactivating BK channels as "BK_i channels" and the resulting whole-cell current as "BK_i current." We term BK channels that exhibit sustained activity "BK_s channels" and the underlying whole-cell current "BK_s current."

BK_i and BK_s channels have also been observed in patches from PC12 cells (Solaro and Lingle, 1992), a rat adrenal chromaffin cell pheochromocytoma cell line (Hatanaka, 1981). As shown in Table 1, excised patches from cultured PC12 cells express about equal proportions of BK_i and BK_s channels, while over time, irrespective of whether cells are grown in NGF or dexamethasone, the relative occurrence of BK_s channels increases.

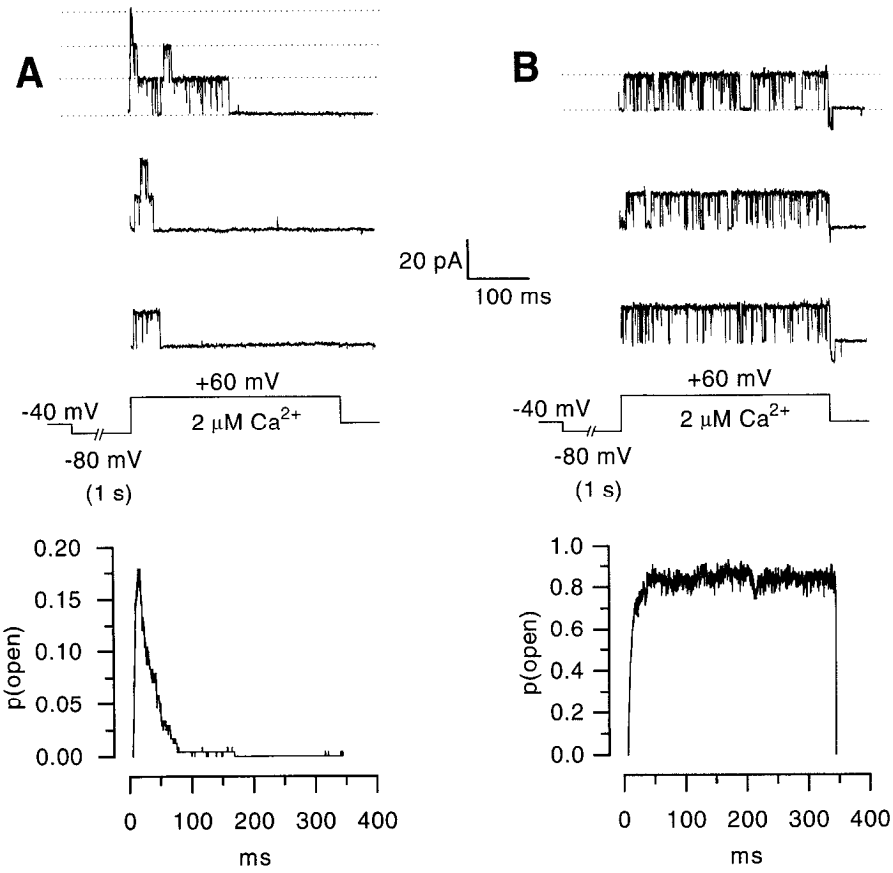

Figure 1. Two kinds of Ca^{2+}- and voltage-dependent K^+ channels in rat chromaffin cells. In *A*, an excised inside-out patch from a rat chromaffin cell was exposed to 2 μM Ca^{2+} and stepped every 3 sec to +60 mV with the voltage protocol shown below the current traces. Up to three channels of about 270 pS conductance are transiently activated. The ensemble average generated from idealized channel openings resulting from 60 such steps is shown below. To identify the number of channels in the patch, the cytosolic face of a patch was briefly exposed to trypsin (0.5 mg/ml) to remove inactivation (Solaro and Lingle, 1992). Based on the total number of channels in a patch, ensemble current amplitude was converted to the probability of being open. There is appreciable resting inactivation in the presence of 2 μM Ca^{2+} at −80 mV, so that the peak p(open) during the step to +60 mV is less than 0.2. In *B*, an excised inside-out patch from another chromaffin cell was stimulated with the same voltage protocol in the presence of 2 μM Ca^{2+}. In this patch, a single noninactivating BK channel is observed. The ensemble average shown below indicates that the single channel open probability exceeds 0.8 at this $[Ca^{2+}]$ and voltage.

Whole-cell recordings reveal either an inactivating or nonnactivating voltage- and Ca^{2+}-dependent current

Depolarizing voltage steps activate a large Ca^{2+}-dependent outward current in both rat (Neely and Lingle, 1992a) and bovine (Marty and Neher, 1985) chromaffin cells. The current–voltage relationship often exhibits a characteristic "hump" or "N-shape" that reflects, in part, the voltage dependence of Ca^{2+} current activation. However, the exact time course and amplitude of this outward K^+ current are complex functions of membrane voltage, submembrane $[Ca^{2+}]_i$, Ca^{2+} current kinetics, and the kinetic properties of the underlying K^+ channels. Consequently, few conclusions about the intrinsic activation and inactivation properties of the Ca^{2+}-dependent K^+ current can be made from the shape of whole-cell currents activated by simple depolarizing voltage steps.

We have found that properties of whole-cell voltage- and Ca^{2+}-dependent K^+ current are better studied using the following protocol: first, cells are depolarized to potentials that activate Ca^{2+} influx through voltage-gated Ca^{2+} channels, thereby loading the cell with Ca^{2+} (Herrington et al., 1995); second, following so-called "loading steps," cells are depolarized further to +81 mV. At +81 mV, near the equilibrium potential for Ca^{2+} (E_{Ca}), Ca^{2+} influx is terminated, while BK current is activated by the positive membrane potential and $[Ca^{2+}]_i$ previously delivered by the loading step. Such a protocol is illustrated in Figure 2, in which a 250 msec step to +1 mV (the loading step) is followed by a step to +81 mV (the test step) either in the presence or absence of extracellular Ca^{2+}. For the cells shown in Figure 2*A* and *B*, the test step to +81 mV that follows a loading step results in the robust activation of Ca^{2+}-dependent current. In Figure 2*A*, Ca^{2+}-dependent current following the loading step decays rapidly to an amplitude similar to that of the voltage-dependent current activated in the absence of extracellular Ca^{2+} (Ca^{2+}_o). In contrast, the Ca^{2+}-dependent current shown in Figure 2*B* decays only slowly over the 500 msec test step. For the moment, we will refer to these currents as presumed BK_i and BK_s currents, respectively. Because both of these currents are absent when Ca^{2+}_o is removed or when the cell is stepped directly to +81 mV without a loading step, both are strictly dependent on Ca^{2+} influx for activation.

Macroscopic currents observed at +81 mV following elevation of cytosolic Ca^{2+} exhibit some variability in the extent of inactivation. Despite this variation, whole-cell current appears to be either predominantly inactivating (BK_i) or predominantly noninactivating (BK_s). For example, despite some variability in inactivation time constants in cells with inactivating current,

Table 1. Number of excised patches containing only BK_i, only BK_s, or both BK_i and BK_s channels

Cell type	BK_i	BK_s	BK_i and BK_s	Total
Rat chromaffin	338 (75.8%)	41 (9.2%)	67 (15.0%)	446
PC12 (untreated)	8 (23.5%)	18 (52.9%)	8 (23.5%)	34
PC12 (+ NGF)	0	4	0	4
PC12 (+ DEX)	1	13	0	14

Numbers in parentheses indicate the percentage of total patches. NGF, nerve growth factor; DEX, dexamethasone. Chromaffin cell patches with only BK_i channels usually contained 3–10 channels, while patches with only BK_s channels contained less than 4 channels.

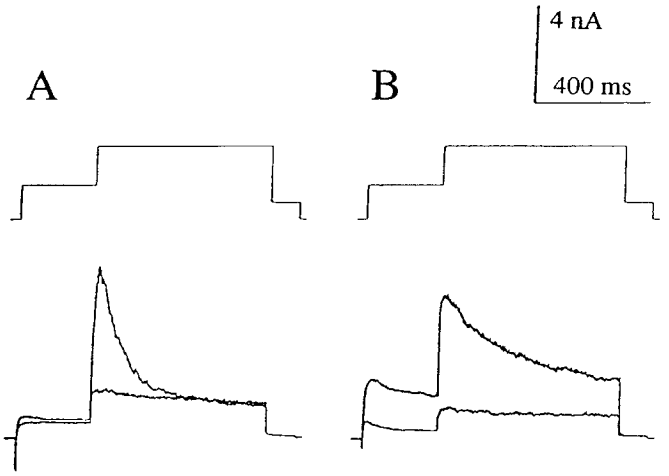

Figure 2. Two kinds of whole-cell Ca^{2+}- and voltage-dependent outward current in rat chromaffin cells. In *A*, currents from a cell with inactivating Ca^{2+}- and voltage-dependent K^+ current (BK_i current) are illustrated, while, in *B*, currents from a cell with a more sustained Ca^{2+}- and voltage-dependent current (BK_s current) are shown. The voltage command protocol is shown on the *top*, and current traces activated either in the presence or absence of extracellular Ca^{2+} are shown on the *bottom*. From a holding potential of −69 mV, each cell was stepped to +1 mV for 250 msec before a subsequent step to +81 mV. In *A*, a completely decaying Ca^{2+}-dependent current is observed during the step to +81 mV, while in *B* there is a substantial amount of more sustained Ca^{2+}-dependent current activated during the step to +81 mV. The differences in the amount of Ca^{2+}-dependent current activated during the step to +1 mV presumably reflect differences in the amount of Ca^{2+} influx in the particular cell and are not correlated with the presence of sustained or decaying Ca^{2+}-dependent current. The amplitude of current activated at +81 mV in the absence of external Ca^{2+} is identical to that activated at +81 mV without a preceding Ca^{2+}-loading voltage step. In *A*, R_s: 9.5 MΩ, 80% compensation; C_m : 5 pF; in *B*, R_s: 12 MΩ, 80% compensated, C_m: 4 pF.

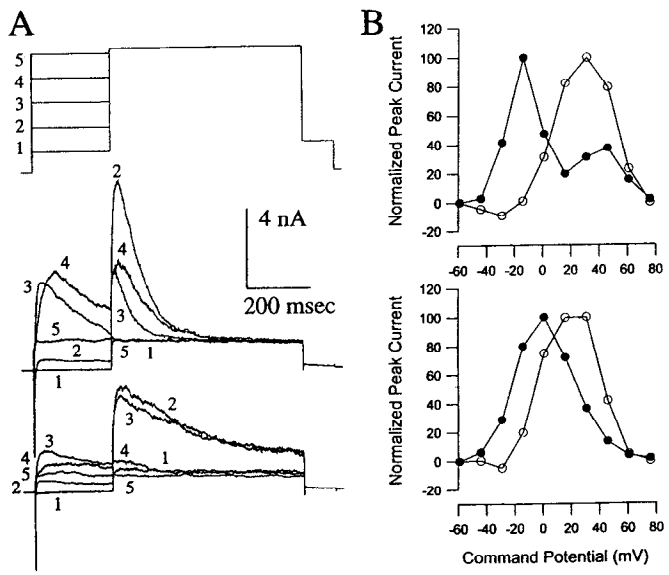

Figure 3. Current–voltage curves in chromaffin cells with either BK_i or BK_s current. In *A*, currents were activated by conditioning steps to potentials from −44 through +76 mV followed by a step to +81 mV, which terminates Ca^{2+} influx. The holding potential was −69 mV. The voltage protocol is displayed on the top and numbers correspond to different command voltages (*1:* −44 mV; *2:* −14 mV; *3:* 16 mV; *4:* 46 mV; *5:* 76 mV). *Middle traces* display currents activated in a cell with BK_i current, while *bottom traces* are from a cell with BK_s current. For the cell with BK_i currents, R_s: 10.4 MΩ; 80% compensated; C_m: 9.4 pF; for the cell with BK_s currents, R_s: 13 MΩ, 80% compensated; C_m: 5.5 pF. In *B*, peak outward current measured either during the conditioning potential (*open circles*) or following the step to +81 mV (*filled circles*) is plotted as a function of the command potential for the sets of currents illustrated in *A*. The *top panel* plots amplitudes from the cell with BK_i current, while the *bottom panel* corresponds to the cell with BK_s current. In both cases, the voltage-dependent K^+ current amplitude at each potential, assuming a linear increase in current between −20 mV and +80 mV (cf. Marty and Neher, 1985), was subtracted in order to obtain the amplitude of current dependent solely on Ca^{2+} influx. Peak current during the conditioning potential exhibits bell-shaped activation typical of Ca^{2+}-dependent current. For the cell with BK_i current, peak current activated at +81 mV following Ca^{2+} influx shows a bimodal shape reflecting increased inactivation of BK current at voltages that produce maximal Ca^{2+} influx.

most cells exhibit BK current which inactivates 95–100% within 300 msec following a step to +81 mV with elevated cytosolic $[Ca^{2+}]$. In contrast, a smaller fraction of cells express BK current that is noninactivating or has inactivated less than 50% within 300 msec following a step to +81 mV. The fractions of cells exhibiting either BK_i or BK_s current, respectively, correlated well with the fraction of patches containing either BK_i or BK_s channels. This issue will be addressed in more detail below (see Fig. 7).

In the next sections, we ask whether the type of BK current observed can be explained by different underlying BK channels or by some difference in the regulation of cytosolic $[Ca^{2+}]$.

Effects of loading step potential on BK current activation

The effect of varying the loading step potential on whole-cell Ca^{2+}- and voltage-dependent current was examined (voltage protocol shown with top traces of Fig. 3*A*). In the first case (Fig. 3*A*, middle traces), test steps to +81 mV that followed loading steps of at least 100 msec duration activated a presumed BK_i current that decayed with a time constant of 50–100 msec. In the second case (bottom traces of Fig. 3*A*), a presumed BK_s current was activated by the test step and decayed more slowly, over hundreds of milliseconds. For each cell, the peak currents activated during both the loading step and during the test step to +81 mV are plotted in Figure 3*B*. Both current measurements exhibit the usual bell-shape characteristic of Ca^{2+}-dependent K^+ current in chromaffin cells (Marty and Neher, 1985; Neely and Lingle, 1992a). Peak current measured during the test step is consistently shifted to more negative potentials relative to the current activated during the loading step. This shift is expected since activation of current at +81 mV reflects only the amount of Ca^{2+} delivered by the loading step, while activation of current during the loading step is limited by the voltage-dependence of BK current activation. For the BK_i current, peak current measured during the step to +81 mV exhibits an anomalous dependence on the loading potential, illustrated by the "notch" in the peak current profile of Figure 3*A*. As shown previously (Herrington et al., 1995), this anomalous reduction of peak current is exaggerated by longer duration loading steps and is more severe for loading potentials that favor Ca^{2+} influx. Reduction of peak current under these conditions is most simply explained by inactivation. Consistent with this result, inactivation of single BK_i channels is favored both by higher $[Ca^{2+}]_i$ and stronger depolarization (Solaro and Lingle, 1992). In sum, these results suggest that in some cells BK current is largely inactivating, while in others the BK current is mostly sustained.

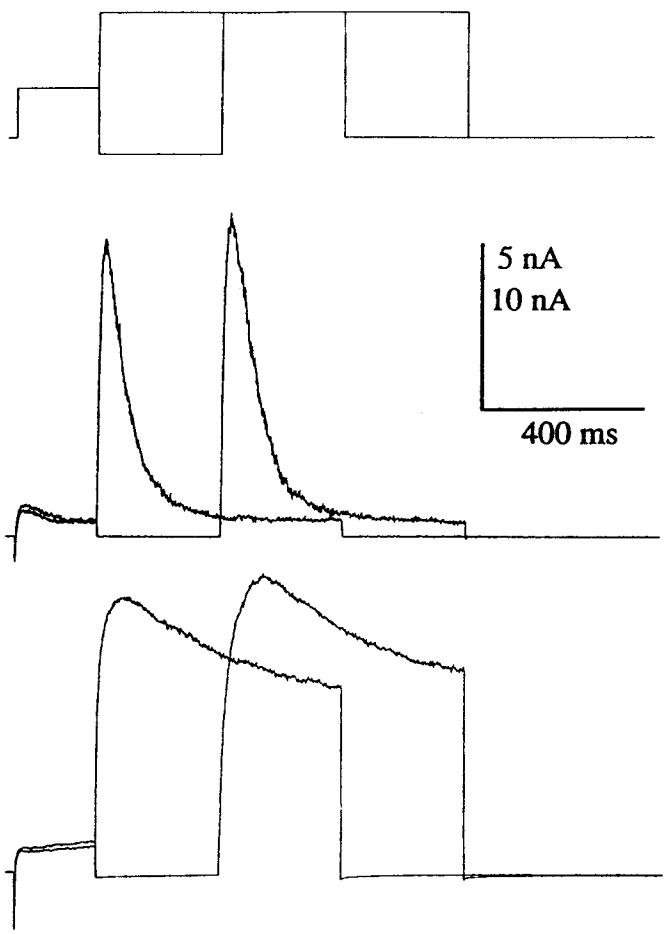

Figure 4. The time course of current at +81 mV following strong Ca^{2+} loading steps reflects BK channel gating behavior and not Ca^{2+} clearance. The *top traces* illustrate the command voltages used to activate current in a cell with BK_i current (*middle traces*) and a cell with BK_s current (*bottom traces*). The command protocol was identical in both cases. From a holding potential of −69 mV, the cells were stepped to −9 mV for 200 msec to elevate cytosolic $[Ca^{2+}]$. The voltage was then stepped to +81 mV with or without an intervening 300 msec recovery period at −89 mV. In both cells, following the recovery period cytosolic $[Ca^{2+}]$ remains sufficiently elevated to cause robust activation of BK current during the subsequent step to +81 mV. The diminution of BK current that occurs during the steps to +81 mV must therefore reflect inactivation of the current, which differs markedly in the two cases. The cells were held at −69 mV for 30 sec between each voltage command sequence. For the cell with BK_i-type current, R_s: 11.5 MΩ; 80% compensated; C_m: 10.8 pF; for the cell with BK_s-type current, R_s: 8 MΩ; 80% compensation; C_m: 8.0 pF.

Whole-cell BK_i current decay reflects inactivation and not Ca^{2+} clearance

We next determined whether the decay of presumed, whole-cell BK_i current does, in fact, reflect inactivation rather than reduction of $[Ca^{2+}]_i$ by cytoplasmic clearance mechanisms. First, $[Ca^{2+}]_i$ was elevated by a 200 msec loading step to −9 mV. Then BK_i current was activated in one of two ways: first, by a test step to +81 mV, which immediately followed the loading step or, second, by a test step that followed a "recovery" step to −89 mV during which cytoplasmic Ca^{2+} might be cleared (Fig. 4). If the BK_i current decay reflected rapid clearance of Ca^{2+} rather than inactivation, there should be no activation of BK current during the test step that followed the recovery step. This was not observed. Instead, BK current activation and inactivation were essentially unchanged, even after recovery steps up to 300 msec in duration. This result indicates that cytosolic $[Ca^{2+}]$ remains elevated during the entire recovery step. Therefore, the decay of BK_i current can only reflect inactivation and not Ca^{2+} clearance.

A similar protocol applied to a cell with a presumed BK_s current is also shown in Figure 4. As for the experiment above, a period of recovery at −89 mV produces little reduction of cytosolic $[Ca^{2+}]$ elevated by a 200 msec loading step to −9 mV. It should also be noted that, despite clear differences in the whole-cell currents illustrated in Figure 4, there is a slow decrease in outward current at +81 mV in the cell with BK_s current, which may reflect some intrinsic inactivation of this current, although at a markedly slower rate.

Effects of increasing the duration of Ca^{2+} influx on BK_i and BK_s currents

The above protocols used long loading steps in order to produce robust elevations of cytosolic $[Ca^{2+}]$. Such elevations presumably saturate cytoplasmic Ca^{2+} clearance mechanisms and allow $[Ca^{2+}]_i$ to stay sufficiently elevated to maximally activate BK current. With smaller Ca^{2+} loads, one might expect the time course of BK currents activated by the test step to reflect, at least in part, the time course of Ca^{2+} clearance mechanisms. BK_s current should decay quickly as Ca^{2+} is cleared following termination of influx. As the Ca^{2+} load is increased, BK_s currents should become progressively prolonged and larger. BK_i current should be similar to BK_s current for small Ca^{2+} loads but should become progressively inactivated as Ca^{2+} loads are increased.

To test these ideas, cytoplasmic $[Ca^{2+}]$ was elevated using progressively longer loading steps before a test step to +81 mV (Fig. 5*A*). For a cell with presumed BK_i current (middle traces of Fig. 5*A*), the peak current activated by the test step increases, while the rate of decay shows little change as the Ca^{2+} load is increased. For a cell with presumed BK_s current, the peak current activated by the test step also increases with longer loading steps, but the decay of current is progressively slowed. Figure 5*B* illustrates currents from the cells shown in *A* recorded with three different loading potentials and a wider range of loading step durations. For BK_i current (left traces), as the duration of the loading step is increased or the loading potential made more positive, peak current is first increased and then suppressed. For the longest loading steps to +11 mV, most BK_i current is inactivated during the loading step so that very little current is activated by the subsequent test step. For a cell with BK_s current (right traces), a larger Ca^{2+} load results in more persistent activation of current during the test step. Thus, following the longest loading step to +11 mV, BK_s current activated at +81 mV shows little decrement over hundreds of milliseconds.

The time constant of BK current decay during the test step was measured and plotted as a function of loading step duration (Fig. 5*C*). For BK_i currents, the time constant gradually increases for loading steps up to about 100 msec in duration, then decreases for longer loading steps. In contrast, the time constant of decay for BK_s currents increases continually with the loading step duration until it becomes imprecisely defined. This is consistent with the idea that the time course of BK current is determined largely by the rise and fall of submembrane $[Ca^{2+}]$ for loading steps of 100 msec or less. For longer loading steps, BK_s current continues to mirror the behavior of submembrane $[Ca^{2+}]$. In contrast, both the increased rate of BK_i current decay and the

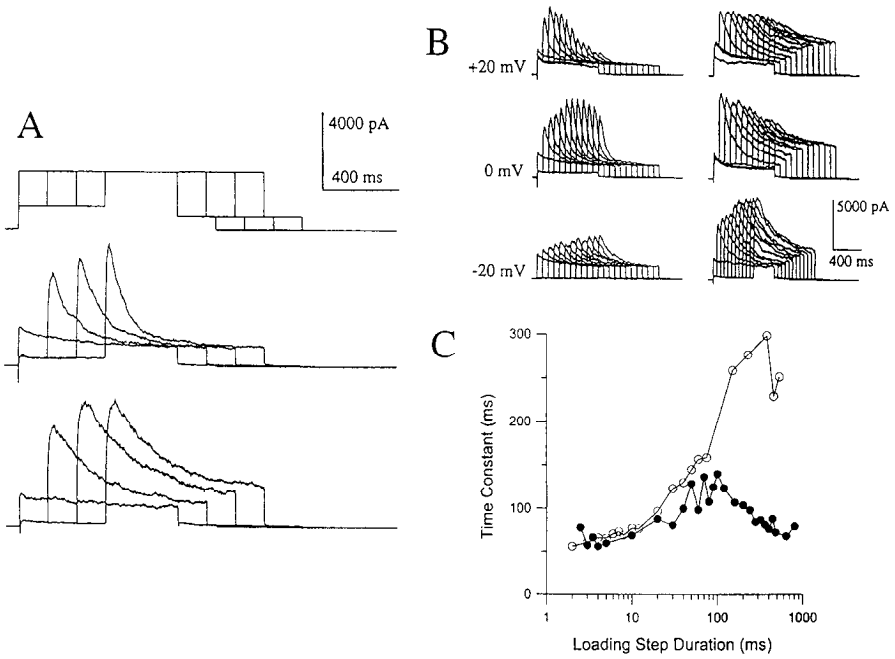

Figure 5. Effect of varying the Ca^{2+} loading step duration on the behavior of BK current activated at +81 mV. In *A*, the *top traces* illustrate command voltage sequences used to activate currents shown in the bottom two sets of traces. The cells were clamped at −69 mV and stepped for different times (0, 150, 300, 450 msec) to −9 mV (*middle traces*) or −29 mV (*bottom traces*) before a subsequent step to +81 mV. The traces activated by stepping directly to +81 mV from −69 mV show current that is strictly voltage dependent, while currents activated at +81 mV following an intervening command step to either −9 or −29 mV reflect current that depends on Ca^{2+} influx. *Middle traces* illustrate current in a cell with inactivating BK current, while *bottom traces* illustrate current in a cell with more sustained BK current. The time between each stimulation was 20 sec. Cells were briefly repolarized to −34 mV before returning to −69 mV at the end of the traces. For the cell with BK_i current: R_s: 9.5 MΩ, 80% compensated; C_m: 5.0 pF; for the cell with BK_s current: R_s: 9.5 MΩ, 80% compensated; C_m: 6.0 pF. In *B*, currents activated by protocols similar to those in *A* are displayed for the same two cells but with three different loading potentials (*top:* +11 mV; *middle:* −9 mV; *bottom:* −29 mV). For the cell with BK_i current (*left traces*), more positive loading potentials result initially in more robust activation of BK current followed by appreciable inactivation of current during the loading step. For the cell with BK_s current (*right traces*), more positive command potentials and longer loading steps results in slower decline of BK current during the steps to +81 mV, indicative of a slower rate of clearance of Ca^{2+} from the cell. The cell with BK_s current may contain a small component of inactivating BK current. In *C*, the time constants of decay of BK current activated at +81 mV following loading steps to −9 mV for a BK_i cell (*filled circles*) and a BK_s cell (*open circles*) are plotted as a function of loading step duration. At loading steps longer than about 500 msec it was not possible to determine meaningful decay rates for the BK_s cell.

suppression of peak current argue that the time course of BK_i current reflects the intrinsic inactivation of the underlying channels. The experiments in Figure 5 also point out that either the cytosolic $[Ca^{2+}]$ falls very little over a 1 sec period following robust $[Ca^{2+}]_i$ elevation, or that $[Ca^{2+}]_i$ remains at a concentration above that which is necessary for maximal activation of BK current at +81 mV.

BK_i and BK_s currents activated when cytosolic $[Ca^{2+}]$ is elevated either by muscarinic receptor activation or by inclusion of Ca^{2+} in the recording pipette

Cytosolic $[Ca^{2+}]$ in rat chromaffin cells can also be elevated by muscarinic receptor-induced release of Ca^{2+} from intracellular stores (Neely and Lingle, 1992b; Herrington et al., 1995). Figure 6 compares currents recorded from cells exhibiting either presumed BK_s (Fig. 6*A,B,C*) or presumed BK_i (Fig. 6*D,E,F*) current during muscarine-induced $[Ca^{2+}]_i$ elevations. In most cells, steps to +81 mV result in large, almost completely inactivating outward currents during the muscarine-induced Ca^{2+} elevation (Fig. 6*D,E*). In such cells, Ca^{2+} loading protocols also give rise to an inactivating, Ca^{2+}-dependent current (Fig. 6*F*). In some cells, however, steps to +81 mV result in large, noninactivating outward currents during the action of muscarine (Fig. 6*A*, slow time base; Fig. 6*B*, representative single sweeps). In such cells, a loading protocol always revealed a Ca^{2+}-dependent, noninactivating current (Fig. 6*C*).

We have also examined the properties of voltage-dependent outward current activated when $[Ca^{2+}]_i$ is elevated by including Ca^{2+} in the recording pipette (Fig.6*G,H*). Outward current was elicited by voltage steps to +81 mV with 4 μM Ca^{2+} in the recording pipette saline and with 200 nM external apamin. Figure 6*G* shows examples of two cells with inactivating current, while Figure 6*H* shows two cells with relatively noninactivating current. Such currents are certainly contaminated by strictly voltage-dependent K^+ currents, but such contamination is minor (Fig. 6*I*). The average peak voltage-dependent K^+ current in cells in which Ca^{2+} is not elevated is typically less than 1 nA at +81 mV. Thus, irrespective of the method of elevating cytosolic $[Ca^{2+}]$, chromaffin cells exhibit BK current that is either largely inactivating or relatively noninactivating.

To compare the phenotypic diversity of BK currents recorded using these different methods, Figure 7 plots histograms of the number of recordings of BK currents with particular inactivation time constants. In Figure 7*A*, the inactivation time constant was measured for whole-cell current recorded when $[Ca^{2+}]_i$ was elevated either by a voltage step to cause Ca^{2+} influx or by muscarine-induced release of stored $Ca^{2+}{}_i$ (Neely and Lingle, 1992b; Herrington et al., 1995). In Figure 7*B*, the inactivation time con-

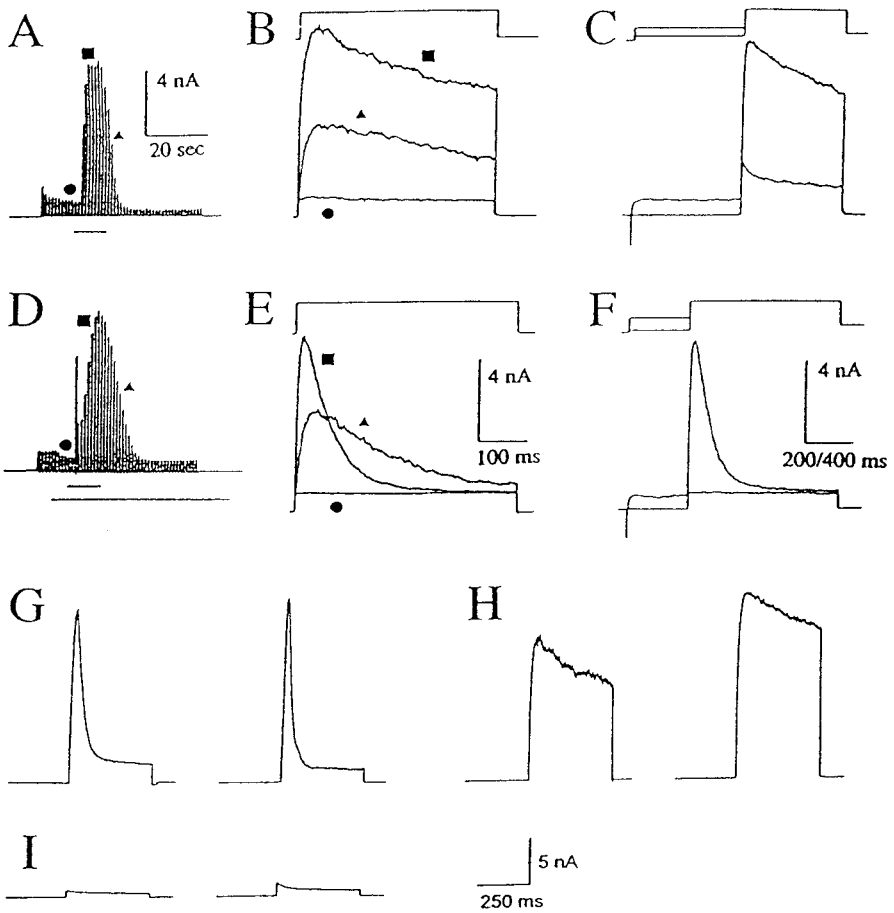

Figure 6. BK_i and BK_s current when $[Ca^{2+}]$ is elevated by release from intracellular stores. Traces in *A*, *B*, and *C* are from a cell that exhibited BK_s type current, while traces in *D*, *E*, and *F* are from a cell with BK_i type current. In *A* and *D*, slow time-base records of membrane current are displayed. Upward deflections correspond to current resulting from command steps to +81 mV applied at 0.5 Hz. During the period indicated by the bar, 50 μM muscarine was applied to each cell, resulting in elevation of cytosolic $[Ca^{2+}]$ and activation of BK current. In *D*, the extracellular saline contained nominally 0 Ca^{2+}. The calibration bar in *A* also applies to *D*. In *B* and *E*, faster time-base records of command steps indicated by the symbols in *A* and *D* are displayed (cell with BK_s current: sweeps 11, 17 and 26; cell with BK_i current, sweeps, 11, 17, and 22). Sweep 11 corresponds to current activated by the voltage step to +81 mV prior to muscarine application. The calibration bar in *E* also applies to *B*. In *C* and *F*, depolarizing steps were used to elevate cytosolic $[Ca^{2+}]$ prior to subsequent steps to +81 mV. In *C*, the holding potential was −69 mV and the cell was stepped to either −49 or −9 mV for 800 msec prior to a step to +81 mV. In *F*, from a holding potential of −69 mV the cell was stepped to either −59 mV or +1 mV for 250 msec before the step to +81 mV. In both cases, the external saline contained 200 nM apamin. The calibration bar in *F* also applies to *C*, with *C* having the slower time base. For the cell with BK_s type current: R_s: 21 MΩ; 80% compensated; C_m: 6 pF; for the cell with BK_i type current: R_s: 8.7 MΩ; 80% compensated; C_m: 6.5 pF. In *G* and *H*, cells were voltage clamped with the standard open-pipette method (Hamill et al., 1981) with 4 μM Ca^{2+} in the pipette. From a holding potential of −63 mV, the voltage-was stepped to +87 mV. *G* shows traces from two cells with inactivating current and *H* shows traces from two cells with relatively noninactivating current. In *I*, traces from two cells with pipette saline containing 80 μM EGTA are shown. In all cases, the external saline contained 200 nM apamin. *G–I* share the same calibration bars.

stant was measured for whole-cell currents recorded when $[Ca^{2+}]_i$ was directly introduced from the recording pipette. When inactivation did not occur or when the inactivation time constant was too slow to be well defined, an entry was placed in the bin corresponding to the largest time constant. For an additional comparison, inactivation time constants for inside-out patches containing exclusively inactivating BK channels were determined from ensemble averages at +60 mV and with 2 or 4 μM $Ca^{2+}{}_i$ (Fig. 7*C*). The faster macroscopic inactivation rates correlate well with the single-channel inactivation rates, and the distributions obtained for each recording method are remarkably similar. With elevated pipette $[Ca^{2+}]$, current inactivated with a time constant of less than 100 msec in 28 of 36 (78%) cells. With the less well-defined elevation of cytosolic $[Ca^{2+}]$ by muscarine or depolarization-elicited influx, 49 of 66 (74%) cells had BK current that inactivated with a time constant of less than 110 msec. This indicates qualitatively the fraction of cells that express BK current that inactivates by over 95% within 300 msec at +81 mV during elevated cytosolic $[Ca^{2+}]$. Together with Table 1, these distributions show that about 75% of the chromaffin cells and patches contain BK currents that inactivate almost completely within 300 msec. The remaining cells or patches exhibited either no inactivation or current that inactivates less than 50% within 300 msec.

These distributions indicate that there is some variability in the range of BK current behavior as defined by the whole-cell inactivation time constant. Although the inactivation rates of most whole-cell currents approach the nearly limiting inactivation rate defined in inside-out patches at +60 mV with $[Ca^{2+}]_i$ greater than 2 μM (Solaro and Lingle, 1992), whole-cell current can range from completely inactivating to noninactivating. For muscarine- or depolarization-induced elevations of cytosolic

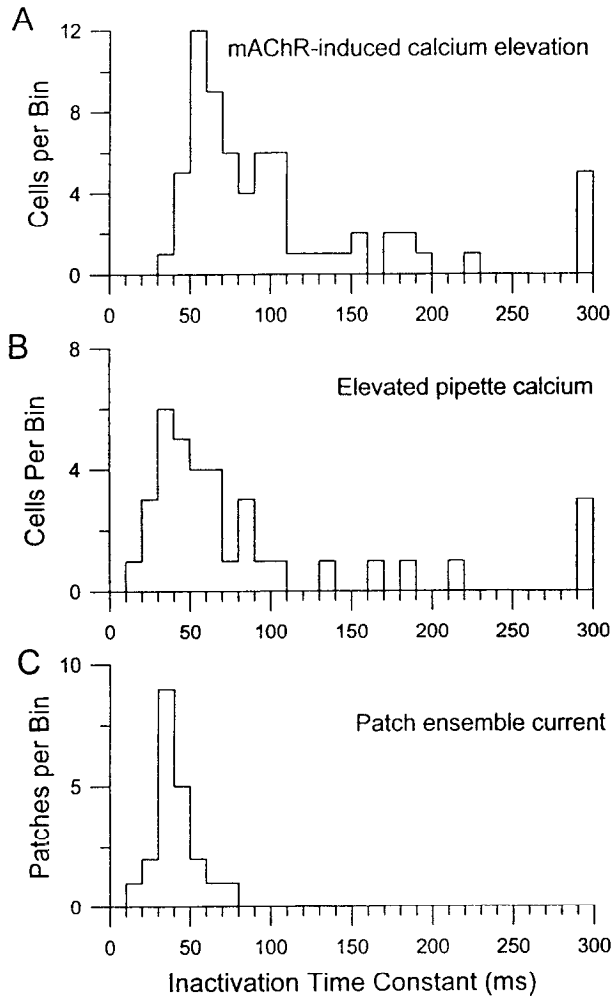

Figure 7. The frequency distribution of BK current inactivation time constants in cells and patches. In *A*, inactivation time constants were measured from the decay of current during a voltage step to +81 mV at the peak of the response to muscarine (e.g., Fig. 6*B* or *E*) or from currents following prolonged depolarizing conditioning steps (e.g., Fig. 6*C* or *F*). In *B*, inactivation time constants were measured for currents activated by voltage steps to +87 mV with pipette $[Ca^{2+}]$ of 4, 10, 20, or 60 μM. For both *A* and *B*, if a cell exhibited no appreciable inactivation, the cell was included in the highest bin. In *C*, inactivation time constants were measured from ensemble currents generated by voltage steps to +60 mV with 2 μM or 4 μM Ca^{2+}_i using inside-out patches held at −40 mV. The plot displays the frequency distribution of patches with different inactivation time constants. Only patches with solely inactivating channels were included in this distribution. See Table 1 for the fraction of patches containing BK_s channels or mixtures of BK_i and BK_s channels. Voltage steps were typically 400 msec in duration.

$[Ca^{2+}]$, it is likely that, in some cells, the elevation of $[Ca^{2+}]_i$ is not large enough to produce maximal inactivation rates of BK current, thereby resulting in the appearance of more slowly inactivating current. However, this is unlikely to be the explanation for the occurrence of totally noninactivating current, since the activation rate of BK current in such cells is not noticeably slower than that for inactivating current. Furthermore, some variability in BK inactivation is still observed when $[Ca^{2+}]$ greater than 4 μM is directly introduced into the cell through the recording pipette. This suggests that variability in macroscopic inactivation behavior may also result from intrinsic variability in the properties of BK current among different cells. However, our observations are generally consistent with the view that the variability in extent of inactivation of BK currents among chromaffin cells does not represent a continuum of BK current behaviors, but rather two qualitatively distinct types of behaviors, predominantly inactivating and predominantly noninactivating, resulting from differential expression of two phenotypic forms of BK channel. Within these two general groupings of current behavior, additional variability may reflect some differential expression of different BK channel variants, heteromultimer formation, BK channel modification, or modulation; however, this issue is not addressed by the present data. Although we have no information about the possible reasons for the two types of BK phenotype, we have noted that some chromaffin cell dispersions appeared to be relatively enriched in cells with BK_s current.

Calcium and voltage-sensitivity of BK_i and BK_s channels

The results above show that BK current in rat chromaffin cells exhibits a broad range of behavior, ranging from completely inactivating to essentially noninactivating. This appears to reflect intrinsic differences in the properties of the BK channels rather than differences in cytosolic $[Ca^{2+}]$ regulation. We next wished to determine whether any other functional aspects of presumed BK_i and BK_s currents might differ. This was approached in three ways: first, by defining the activation rates of BK channels in excised inside-out patches; second, by examination of BK channel deactivation rates; and, third, by comparing the fractional activation of whole-cell BK_i and BK_s current during voltage steps when Ca^{2+} is introduced into the cell through the recording pipette.

Activation and deactivation of BK_i and BK_s channels. The activation time course of single BK_i and BK_s channels recorded in excised inside-out patches was compared using the protocol shown in Figure 8*A* and *B*. Ensemble average currents were generated and fitted by a Hodgkin-Huxley model (see Materials and Methods) to obtain estimates of the rate and cooperativity of activation. BK_i and BK_s channels showed no obvious differences in these parameters. At +60 mV and 2 μM Ca^{2+}_i, activation time constants were 10.2 ± 4.5 msec (mean ± standard deviation, n = 7) for BK_i channels, and 8.7 msec (mean, n = 2) for BK_s channels. Estimates of cooperativity were 1.06 ± 0.30 for BK_i channels, and 0.70 for BK_s channels. Thus, we expect activation of BK_i and BK_s channels to follow a similar time course immediately following short-duration depolarizations with elevated submembrane $[Ca^{2+}]$.

To compare deactivation, patches containing either BK_i or BK_s channels were briefly stepped to +60 mV and then repolarized to −40 mV in the presence of 2 μM Ca^{2+}_i (Fig. 8*C*). Ensemble tail currents were generated, and deactivation time constants were measured by fitting an exponential function to the current decay. Deactivation of BK_i channels was best fitted by two exponential components (τ_{fast} = 2.4 ± 0.46 msec (mean ± SEM); τ_{slow} = 12.0 ± 3.0 msec; fraction slow = 0.6; n = 6) while a single exponential could adequately describe BK_s channel deactivation (τ = 2.0 ± 0.3 msec; n = 4). BK_s channels deactivated with a time course that was similar to the fast component of BK_i deactivation; however, there was no evidence for a slower second component.

Voltage and Ca^{2+}-dependence of whole-cell BK current. A second component of deactivation may represent an open state unique to BK_i channels and suggests that some differences in steady-state Ca^{2+} and voltage dependence of BK_i and BK_s channel p(open) might exist. Single-channel experiments have shown that BK_i channels exhibit pronounced steady-state inactivation

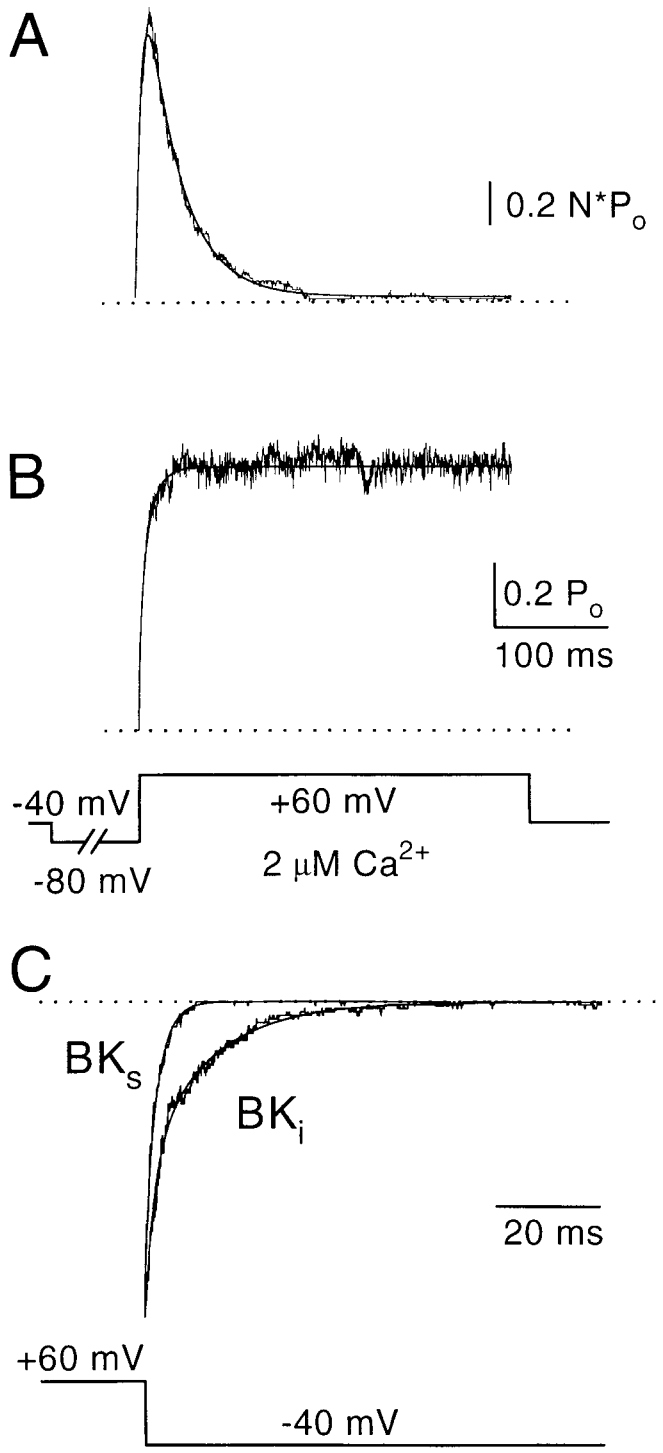

Figure 8. The time course of activation for BK_i and BK_s channels is similar, but deactivation time course differs. BK_i channels (*A*) or BK_s channels (*B*) in inside-out patches were held at −40 mV and stepped to +60 mV every 3 sec using the voltage protocol shown. *A* and *B* show the time course of P_o, calculated by averaging idealized records. These traces were fitted with a Hodgkin-Huxley model for inactivating current (see Materials and Methods) as shown by *solid lines* superimposed on the averages. The patch in *A* contained at least five BK_i channels and 70 sweeps were averaged. The patch in *B* contained a single BK_s channel, and 110 sweeps were averaged. Parameters of the fits are given in the text. Because the exact number of inactivating channels for the patch shown in *A* was unknown, $N*P_o$ rather than P_o was calculated, where N is the number of channels in the patch. *Dotted lines* are drawn at zero P_o. In *C*, inside-out patches containing either BK_i or BK_s channels were held at −40 mV, depolarized to +60 mV for 10 msec, and then repolarized to −60 mV for 100 msec. The traces (labeled *BK_s* and *BK_i*) show average P_o during repolarization and were generated by averaging idealized opening and closings after repolarization. Maximal P_o is plotted downward to emphasize deactivation and scaled to the same peak amplitude to facilitate comparison. The time course of BK_i repolarization was best fit by the sum of two exponentials ($A_{fast} * \exp(-t/\tau_{fast}) + A_{slow} * \exp(-t/\tau_{slow})$), while a single exponential [$A * \exp(-t/\tau)$] could sufficiently describe BK_s repolarization. Fits are shown as *solid lines* superimposed on the traces, and the time constants are as shown. Additional parameters are given in the text. The *dotted line* indicates zero P_o.

with $[Ca^{2+}]_i$ of 2 μM and above (Solaro and Lingle, 1992; Herrington et al., 1995). Furthermore, both the time course of activation and peak BK_i current during a voltage step is limited by the appreciable inactivation that occurs during the rising phase of the current. These limitations preclude a simple comparison of the Ca^{2+} and voltage dependence of BK_i and BK_s steady-state open probability. Thus, it was desirable to have an independent method to compare the Ca^{2+} and voltage dependence of BK current. To accomplish this, BK current activation was examined in whole-cell recordings in which 4 μM $[Ca^{2+}]$ was directly introduced into the cell from the recording pipette.

Single-channel experiments indicate that near +87 mV with $Ca^{2+}{}_i$ at concentrations of 4 μM and higher, the open probability of BK channels is near maximal. Therefore, peak whole-cell current measured at +87 mV with a comparable $[Ca^{2+}]_i$ would provide an indication of the maximum available BK current at the time of a voltage step. The fraction of available BK channels activated by a conditioning voltage step prior to a step to +87 mV can then be estimated from the amount of current active immediately following the step to +87. The ratio of the current immediately following a step to +87 mV to the peak current activated at +87 mV provides an estimate of the fractional activation of BK current at the conditioning voltage. As shown in Figure 9*A*, when the membrane potential is stepped from the conditioning voltage to +87 mV, there is an instantaneous, ohmic step of current that reflects current activated during the conditiong step. This is followed by slower, additional activation due to the stronger test pulse. Thus, the ratio of instantaneous-to-peak current measured during the test pulse when plotted against the conditioning voltage estimates the voltage dependence of BK current activation (Fig. 9*B*). This procedure will overestimate the fractional activation at any conditioning potential by the amount of inactivation that occurs between the instantaneous and peak current at +87 mV. Since activation at +87 mV is rapid compared to inactivation, this error is minor. A second error will result from the contamination of traces by voltage-dependent K^+ current. Since the amount of voltage-dependent K^+ current at +87 mV is typically less than 10% of the peak BK current, this error also should be minor.

Figure 9*A* illustrates instantaneous and peak outward currents activated from two conditioning potentials with 4 μM $Ca^{2+}{}_i$ for a cell with predominantly BK_i current (BK_i cell) and a cell with predominantly BK_s current (BK_s cell). Figure 9*B* plots the normalized G-V curves obtained in this fashion for six BK_i cells and five BK_s cells. The voltage of half activation (V_{50}) at 4 μM for BK_i cells was 48.2 ± 1.4 mV with a slope factor of 13.1 ± 1.3 mV (fitted value with 90% confidence limit). For BK_s cells, the V_{50} was 54.1 ± 2.2 mV with a slope factor of 14.8 ± 2.1 mV. The similarity of these values supports the idea that the Ca^{2+} and voltage dependence of activation does not differ ap-

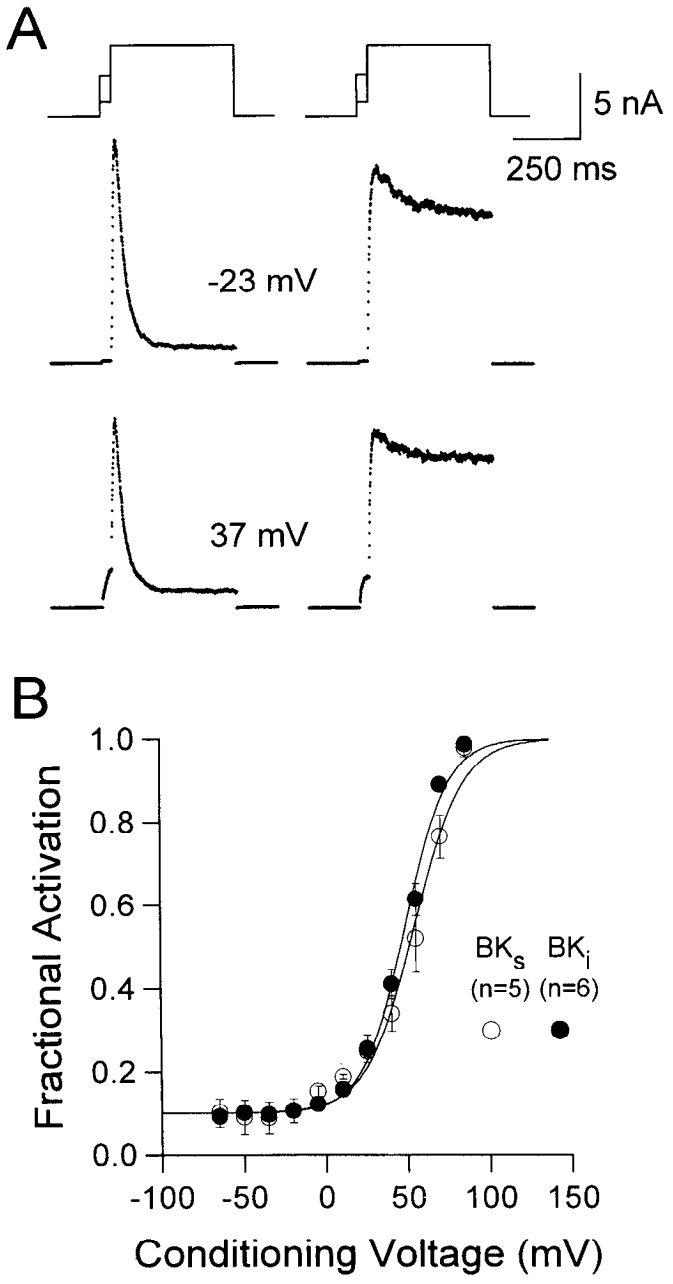

Figure 9. Ca^{2+}- and voltage dependence of BK_i and BK_s current measured in whole-cell recordings with defined pipette $[Ca^{2+}]$. In *A*, on the *top*, the voltage-protocol used to activate BK current during a whole-cell recording with 4 μM Ca^{2+} is shown. Typical currents activated by the voltage steps are shown for a BK_i cell (on the *left*) and for a BK_s cell (on the *right*). In both cases, following a depolarizing conditioning step to the indicated potentials, when the voltage is stepped to +87 mV, there is an ohmic step of current followed by a slower additional activation of current. For the BK_i cell, the level of current after inactivation of BK current provides an indication of contaminating voltage-dependent K^+ current. Small depolarizing conditioning steps result in small ohmic steps followed by a large additional activation at +87 mV. For the cell with BK_i current: R_s: 6.2 MΩ; C_m: 6.5 pF; 80% compensated. For the cell with BK_s current: R_s: 6.7 MΩ; C_m: 7.0 pF; 80% compensated. In *B*, the instantaneous current amplitude was in each case normalized to the peak current activated at +87 mV. This value reflects the fractional activation of maximal activatable BK current at the particular conditioning potential. Points correspond to estimates from six BK_i cells and five BK_s cells. Each set of values was fit with a single Boltzmann function that included a voltage-independent nonzero term. Fitted values are provided in the text. The voltage-independent term for each fit represents the amount of BK current activated by the voltage step to +87 mV during the first sampling interval.

preciably between BK_i and BK_s currents in rat chromaffin cells. This may seem surprising, given the differences in deactivation behavior; however, it is possible that subtle differences in the Ca^{2+} dependence of activation are overlooked by this method.

Sensitivity of BK_i and BK_s currents to TEA, charybdotoxin, and iberiotoxin

Single BK_i and BK_s channels exhibit a similar sensitivity to extracellular TEA, with 50% blockade between 200 and 300 μM (Yellen, 1984; Solaro and Lingle, 1992). Whole-cell BK_i and BK_s currents measured at +81 mV were also blocked to a similar degree by TEA. TEA (300 μM) blocked BK_s currents by 54.2 ± 6.5% (mean ± SD; n = 3) and BK_i currents by 54.5 ± 5.9 (n = 10).

BK currents are also known to be sensitive to the scorpion toxins, charybdotoxin (CTX) (Miller et al., 1985) and iberiotoxin (IBX) (Candia et al., 1992; Giangiacomo et al., 1992), although resistant channels from brain have been described (Reinhart et al., 1989). The sensitivity of rat chromaffin cell BK current to CTX and IBX was examined both in outside-out patches and in whole-cell recordings. Both BK_i and BK_s current were sensitive to 100 nM CTX (not shown); however, while BK_s current was usually blocked completely, block of BK_i current was much more variable. Similar results were obtained using IBX. Currents that were resistant to CTX were similarly resistant to IBX. Possible explanations for variable toxin sensitivity will be examined in more detail elsewhere (manuscript in preparation).

Current clamp behavior of cells expressing BK_i and BK_s currents

The functional role of BK channels in chromaffin cells has not been directly demonstrated; moreover, the functional significance of two BK channel types is not clear. To address this issue, cells expressing either BK_i or BK_s currents were examined under current clamp in the presence of apamin so that all voltage-independent, Ca^{2+}-activated K^+ current was abolished. Single-action potentials were elicited by brief, superthreshold, depolarizing current injections. As shown in Figure 10*A*, the basic action potential waveform is similar for a cell with BK_i current and one with BK_s current, although there is some tendency for cells with BK_i current to have more pronounced afterhyperpolarizations. In both cases, removal of extracellular Ca^{2+} slows the second half of the repolarization phase of the action potential, suggesting that BK current is activated only during the later phases of repolarization. On average, however, the effect of Ca^{2+} removal was smaller in BK_s cells than in BK_i cells. Since removal of Ca^{2+} can produce a variety of effects unrelated to reduction of BK current activation, we attempted to more selectively remove the contribution of BK current to action potential repolariziation using CTX. Although CTX is less effective on BK_i current than on BK_s current, blockade of BK_i current by 100 nM CTX typically exceeds 50% without affecting voltage-dependent K^+ current. As this concentration, CTX results in a marked slowing of the action potential repolarization in BK_i cells (Fig. 10*B*). These results show that BK current is activated during repolarization and the effect of BK current is more pronounced in BK_i cells.

We next wished to examine whether BK_i and BK_s cells showed differences in their ability to fire action potentials repetitively. Both Na^+ and Ca^{2+} currents contribute to chromaffin cell action potentials (Kidokoro and Ritchie, 1980), and during repetitive firing the relative contribution of Na^+ current to chro-

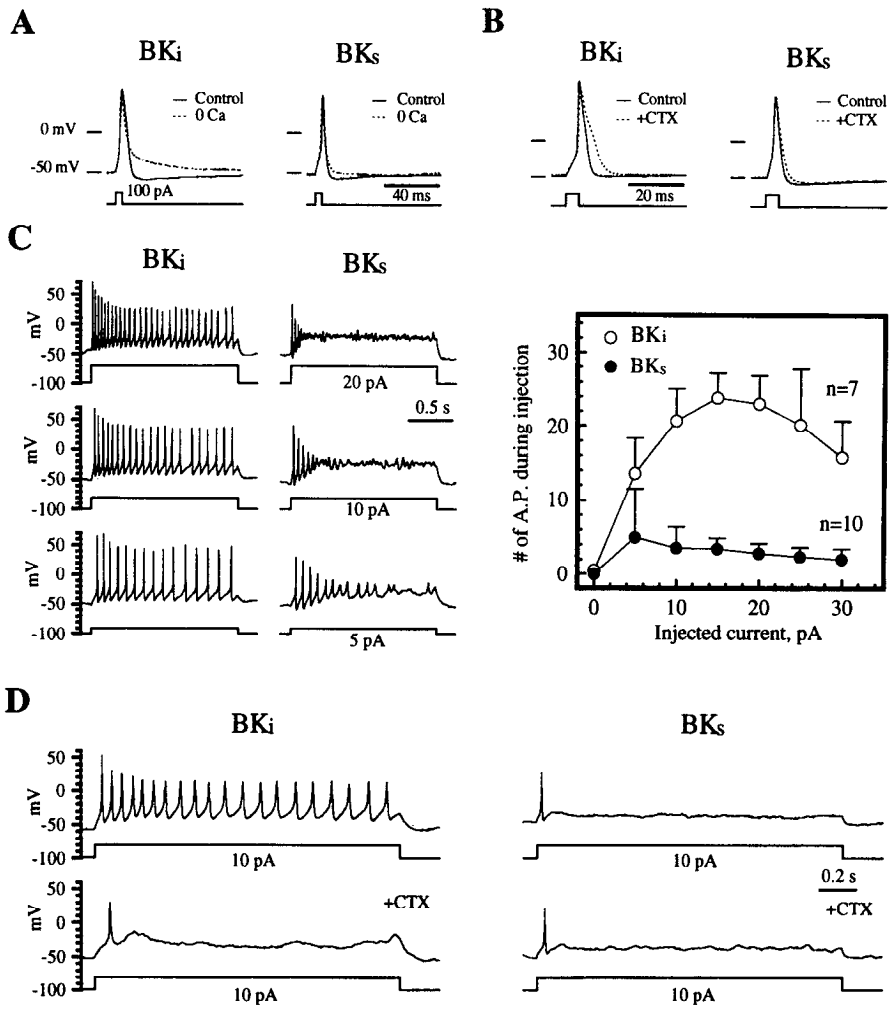

Figure 10. BK current contributes to action potential repolarization and influences repetitive firing. In *A*, representative action potential waveforms elicted by brief depolarizing current pulses are shown for a BK_i cell (*left*) and a BK_s cell (*right*). Traces are also shown for the action potential waveforms elicited in nominally 0 Ca^{2+} saline. For traces in this figure, the external saline contained 200 nM apamin. In *B*, the action potential waveform elicited in a BK_i (*left*) and a BK_s (*right*) cell in the absence and presence of 100 nM CTX. Although BK_i current is less sensitive to CTX than BK_s current, sufficient block occurs at 100 nM CTX to produce marked action potential prolongation. The action potentials were elicited from a holding potential of about −50 mV. In *C*, 2 sec depolarizing current pulses were applied to a BK_i cell (on the *left*) and a BK_s cell (on the *right*). The BK_i cell fires tonically over a range of injection currents, while the BK_s cell responds with only a few action potentials. The plot on the right of *C* shows the average number of action potentials during the 2 sec of current injection plotted as a function of the amount of injected current for each type of cell. In *D*, the effect of 100 nM CTX on the responses of a BK_i (*left*) and a BK_s cell (*right*) to depolarizing constant current injection are shown.

maffin cell action potentials typically diminishes due to inactivation. As a consequence, marked changes in action potential amplitude and duration can occur, depending on whether an action potential arises exclusively from Ca^{2+} influx or from both Na^+ and Ca^{2+} influx. As one measure of the ability to fire repetitively, the number of action potentials with peak amplitude exceeding 0 mV during a 2 sec period of depolarizing current injection was determined (Fig. 10*C*). Qualitatively, the ability of a cell to fire repetitively during constant current injection differs markedly between BK_i and BK_s cells. In particular, over a rather broad range of injected current, BK_i cells are able to fire repetitively during a 2 sec depolarizing pulse. These action potentials exceed 0 mV and are of short duration, characteristic of action potentials with a prominent Na^+ current component. In contrast, BK_s cells may fire repetitively at the smallest levels of injected current. However, the peak amplitude of action potentials in BK_s cells rapidly falls to voltages below 0 mV and the action potential duration becomes markedly prolonged, characteristic of action potentials arising predominantly from Ca^{2+} currents. In the right panel of Figure 10*C*, the number of action potentials over a 2 sec period that exceed a peak amplitude of 0 mV is plotted as a function of the amount of injected current. This plot indicates that BK_i cells are more competent to repetitively fire action potentials, at least during block of SK current by apamin.

If the properties of a particular BK current variant were important for determining the ability of chromaffin cell to fire repetitively, blockade of BK channels should alter the electrical firing behavior of those chromaffin cells for which BK current is critical. The CTX results described above suggested that the contribution of BK current to repolarization was more substantial in BK_i cells than in BK_s cells. Given the slower deactivation rate of BK_i channels, it seemed possible that BK_i current may give rise to a more prolonged afterhyperpolarization in BK_i cells, perhaps facilitating recovery of voltage-dependent Na^+ channels from inactivation. If BK_i current were in some way permissive for repetitive firing, one would predict that reduction of BK_i current by CTX should convert a tonically firing BK_i cell into a phasically firing cell. In contrast, CTX would be expected to have little effect on the response of BK_s cells to depolarizing current injection. This expectation is confirmed in Figure 10*D*. This experiment clearly shows that functional BK_i current is critical for the ability of chromaffin cells to fire repetitively.

Although both BK channel types contribute to action potential repolarization in different rat chromaffin cells, the faster deactivation kinetics of BK_s current apparently minimize the contribution of BK_s current to any afterhyperpolarization in BK_s cells. In contrast, the slower deactivation kinetics of BK_i current are apparently sufficient to permit a slightly more substantial afterhyperpolarization that is required for the subsequent initiation of action potentials.

Other similarities and differences between cells expressing BK_i or BK_s currents

The selective expression of either a noninactivating or inactivating BK channel by particular rat chromaffin cells raises the possibility that other differences between the two types of cells may exist. However, we find no other membrane current correlated with the presence of BK_i or BK_s current. These currents include voltage-dependent Na^+, voltage-dependent K^+, SK, and a muscarine-activated nonselective cation current (Ding and Lingle, unpublished observations).

Discussion

The primary finding in this article is that rat chromaffin cells exhibit considerable functional heterogeneity in the properties of the Ca^{2+}- and voltage-activated BK currents they express. About 75–80% of cells studied expressed mostly inactivating BK_i current, while the remainder express a sustained or more slowly inactivating BK_s current. Thus, BK current phenotype is strongly segregated among chromaffin cells. The presence of either BK_i or BK_s current is not correlated with any other electrophysiological property of chromaffin cells, including the type or amount of Na^+ current, voltage-dependent K^+ current, apamin-sensitive SK current, or nicotinic acetylcholine receptor-gated current expressed, or the ability of muscarine to release Ca^{2+} from intracellular stores or activate a nonselective cation current.

Besides differing in inactivation, BK_i and BK_s channels exhibit different deactivation behavior. However, there are no obvious differences in the ranges of $[Ca^{2+}]_i$ and voltage required to activate BK_i and BK_s currents or in the rates of activation. This suggests that the two currents are activated by similar physiological stimuli. This assertion, though, must be tempered by the limited range of conditions over which activation was examined.

Using the BK currents as an assay for submembrane $[Ca^{2+}]$, we demonstrate that the time course of $[Ca^{2+}]_i$ elevation produced by depolarization proceeds in a qualitatively similar fashion, regardless of the type of BK current present. Furthermore, clearance of $Ca^{2+}{}_i$ following muscarine-induced release of intracellular stores or following short or long loading pulses appears to proceed in a qualitatively similar fashion in chromaffin cells with different BK currents. These considerations would suggest that both BK_i and BK_s channels respond similarly to short duration $[Ca^{2+}]_i$ elevations, presumably like those associated with activation of Ca^{2+} channels during action potentials. With prolonged $[Ca^{2+}]_i$ elevation, differences in inactivation between the two BK channel types would become more important (Herrington et al., 1995).

Molecular components responsible for BK current diversity in chromaffin cells

Mammalian BK channels are now thought to arise from the expression of a gene (Butler et al., 1993) homologous to the *Slo* locus of *Drosophila* (Adelman et al., 1992). Diversity in BK channel function may arise from alternatively spliced variants (Adelman et al., 1992; Butler et al., 1993) or by association with accessory subunits (Knaus et al., 1994). We have identified two alternatively spliced *Slo* variants from rat chromaffin cell and PC12 cDNA libraries (Saito et al., 1994). Although a molecular mechanism of inactivation has not been identified, these initial results indicate that multiple BK channel subunits may be available for expression within chromaffin cells.

Diversity in BK current phenotype could arise from a number of mechanisms. First, the two types of currents could result from expression of two distinct BK channels, each composed of entirely distinct subunits. Second, channels could be assembled by heteromultimeric combinations of at least two channel subunit types (Isacoff et al., 1990; Covarrubias et al., 1991), one of which confers inactivation. Third, distinct BK current phenotypes may result from identical channel proteins, which are differentially altered by some posttranslational process. These issues are currently being addressed.

BK channel variants and electrical excitability

The behavior of chromaffin cell membrane potential depends on the type of BK current present. Specifically, BK_i current appears to permit chromaffin cells to fire action potentials repetitively over a broad range of injected depolarizing currents. Although any pattern of voltage behavior reflects a complex interplay of a number of ionic conductances, these results argue strongly that the type of BK current expressed critically determines the type of firing pattern observed. Thus, cells that express BK_i current respond to depolarizing stimuli with a tonic firing pattern, while BK_s cells exhibit a phasic firing pattern. It is interesting to note that phasic and tonic firing patterns have been found in guinea pig adrenal chromaffin cells (Holman et al., 1994).

Consistent with the proposed role of BK channels in many cell types (Pennefather et al., 1985; Lancaster and Adams, 1986; Lang and Ritchie, 1987, 1990), both BK_i and BK_s currents contribute to action potential repolarization in chromaffin cells. However, the their contributions to repolarization appear to differ. BK_i current produces more prolonged afterhyperpolarizations, thereby permitting repetitive firing in chromaffin cells. This is a new functional role for a BK-type current, and, interestingly, it stems not from the channel's most remarkable feature, i.e., inactivation, but rather from its slower deactivation kinetics.

One might therefore ask what the functional significance of inactivation is, given that no obvious inactivation appears to occur during a series of action potential waveforms (Ding, unpublished observations). Previous work has demonstrated that significant inactivation of BK_i current does occur following muscarine-induced elevation of cytosolic $[Ca^{2+}]$ (Herrington et al., 1995). At membrane potentials in the range of -40 to -50 mV, muscarine-induced release of Ca^{2+} from cytosolic stores can result in inactivation of over half the BK_i current (Herrington et al., 1995), while a similar elevation in a cell with BK_s current results in a small but sustained activation of outward current. Thus, during and just after a response to muscarine, a cell with BK_i current might switch from a tonic to a phasic pattern of firing, while firing patterns for cells with BK_s current would be relatively unchanged. We therefore propose that the magnitude of BK current inactivation during muscarine-induced elevation of cytosolic $[Ca^{2+}]$ may be so large that depolarizing stimuli following the muscarine-induced response may be less able to produce repetitive firing. This would effectively convert a cell capable of firing tonically in response to depolarizing stimuli to one that may only fire phasically.

Some fraction of rat chromaffin cells express macroscopic current, which appears to contain both inactivating and noninactivating components. If such current results in large measure from the expression of both inactivating and noninactivating BK channels, how might such cells behave under current clamp? During constant current injection we would expect that the presence of BK_i current would act in a phenotypically dominant

fashion and permit repetitive action potential firing. The presence or absence of slowly deactivating BK_i current would be the primary determinant of how a cell responds during current injection.

Implications for secretory behavior

The different patterns of firing behavior between BK_i and BK_s cells may be important for the response to secretagogues. In particular, cells with different types of BK current may show quite different patterns of action potential firing given similar depolarizing stimuli. Thus, the secretory response to the same depolarizing secretagogue might differ between the two types of cells. The differences between cells with BK_i and BK_s current are also interesting in light of the possibility that secretion of particular catecholamines may be differentially regulated (Douglass and Poisner, 1965; Vollmer et al., 1992). In fact, the percentage of rat chromaffin cells that express predominantly BK_i-type current behavior corresponds well with the 80% of rat chromaffin cells known to express phenylethanolamine-N-methyltransferase (Verhofstad et al., 1985; Tomlinson et al., 1987; our unpublished observations), the enzyme required for synthesis of epinephrine (EPI) from norepinephrine (NE). At present, physiological differences between distinct chromaffin cell subpopulations have not been described. It will therefore be interesting to determine whether EPI-secreting chromaffin cells express mostly BK_i channels and NE-secreting chromaffin cells express predominantly BK_s channels.

The results presented here show that a grossly homogeneous cell population expresses a current with a remarkably diverse range of functional characteristics. If it turns out that a unique physiological consequence is associated with the selective expression of a particular BK current phenotype, it would provide one of the clearest examples of a cell's ability to express a particular type of K^+ channel tailored for a particular functional role.

References

Adams PR, Constanti A, Brown DA, Clark RB (1982) Intracellular calcium activates a fast, voltage-sensitive K^+ current in vertebrate sympathetic neurones. Nature 296:746–749.

Adelman JP, Shen KZ, Kavanaugh MP, Warren RA, Wu YN, Lagrutta A, Bond CT, North RA (1992) Calcium-activated potassium channels expressed from cloned complementary DNAs. Neuron 9:209–216.

Butler A, Tsunoda S, McCobb D, Wei A, Salkoff L (1993) mSlo, a complex mouse gene encoding "maxi" calcium activated potassium channels. Science 261:221–224.

Candia S, Garcia ML, Latorre R (1992) Iberiotoxin: a potent blocker of the large-conductance Ca^{2+}-activated K^+ channel. Biophys J 63: 583–590.

Covarrubias M, Wei A, Salkoff L (1991) Shaker, Shal, Shab and Shaw express independent K^+ current systems. Neuron 7:763–773.

Douglass WW, Poisner AM (1965) Preferential release of adrenaline from the adrenal medulla by muscarine and pilocarpine. Nature 208: 1102–1103.

Fenwick EM, Fajdiga PB, Howe NBS, Livett BG (1978) Functional and morphological characterization of isolated bovine adrenal medullary cells. J Cell Biol 76:12–30.

Giangiacomo KM, Garcia ML, McManus OB (1992) Mechanism of iberiotoxin block of the large-conductance calcium-activated potassium channel from bovine aortic smooth muscle. Biochemistry 31: 6719–6727.

Hamill OP, Marty A, Neher E, Sakmann B, Sigworth FJ (1981) Improved patch-clamp techniques for high resolution recording from cells and cell-free membrane patches. Pflugers Arch 381:85–100.

Hatanaka H (1981) Nerve growth factor-mediated stimulation of tyrosine hydroxylase activity in a clonal rat pheochromocytoma cell line. Brain Res 222:225–233.

Herrington J, Solaro CR, Neely A, Lingle, CJ (1995) Suppression of calcium- and voltage-activated current by muscarinic acetylcholine receptor activation in rat chromaffin cells. J Physiol (Lond) 485:297–318.

Hille B (1992) Ionic Channels of excitable membranes. Sunderland, MA: Sinauer.

Hodgkin AL, Huxley AF (1952) A quantitative description of membrane current and its application to conduction and excitation in nerve. J Physiol (Lond) 108:37–77.

Holman ME, Coleman HA, Tonta MA, Parkington HC (1994) Synaptic transmission from splanchnic nerves to the adrenal medulla of guinea-pigs. J Physiol (Lond) 478:115–124.

Horn R, Marty A (1988) Muscarinic activation of ionic currents using a new whole-cell recording method. J Gen Physiol 92:145–159.

Isacoff EY, Jan YN, Jan LY (1990) Evidence for the formation of heteromultimeric potassium channels in *Xenopus* oocytes. Nature 345:530–534.

Kidokoro, Y, Ritchie, AK (1980) Chromaffin cell action potentials and their possible role in adrenaline secretion from rat adrenal medulla. J Physiol (Lond) 307:199–216.

Kilpatrick DL, Ledbetter FH, Carson KA, Kirshner AG, Slepetis R, Kirshner, N (1980) Stability of bovine adrenal medulla cells in culture. J Neurochem 35:679–692.

Knaus HG, Garcia-Calvo M, Kaczorowski GJ, Garcia ML (1994) Subunit composition of the high conductance calcium-activated potassium channel from smooth muscle, a representative of the mSlo and slowpoke family of potassium channels. J Biol Chem 269:3921–3924.

Lancaster B, Adams PR (1986) Calcium-dependent current generating the afterhyperpolarization of hippocampal neurones. J Neurophysiol 55:1268–1292.

Lancaster B, Nicoll RA (1987) Properties of two calcium-activated hyperpolarizations in rat hippocampal neurones. J Physiol (Lond) 389:183–203.

Lang, DG, Ritchie, AK (1987) Large and small conductance calcium-activated potassium channels in the GH_3 anterior pituitary cell line. Pflugers Arch 410:614–622.

Lang DG, Ritchie AK (1990) Tetraethylammonium blockade of apamin-sensitive and insensitive Ca^{2+}-activated K^+ channels in a pituitary cell line. J Physiol (Lond) 425:117–125.

Livett BG (1984) Adrenal medullary chromaffin cells *in vitro*. Physiol Rev 64:1103–1161.

Marty A (1981) Ca-dependent K channels with large unitary conductance in chromaffin cell membranes. Nature 291: 497–500.

Marty A, Neher E (1985) Potassium channels in cultured bovine adrenal chromaffin cells. J Physiol (Lond) 367:117–141.

Miller C, Moczydlowski E, Latorre R, Phillips M (1985) Charybdotoxin, a protein inhibitor of single Ca^{2+}-activated K^+ channels from mammalian skeletal muscle. Nature 313:316–318.

Neely A, Lingle CJ (1992a) Two components of calcium-activated potassium current in rat adrenal chromaffin cells. J Physiol (Lond) 453: 97–131.

Neely, A, Lingle, CJ (1992b) Effects of muscarine on single rat adrenal chromaffin cells. J Physiol (Lond) 453:133–166.

Park, YB (1994) Ion selectivity and gating of small conductance Ca^{2+}-activated K^+ channels in cultured rat adrenal chromaffin cells. J Physiol (Lond) 481:555–570.

Pennefather P, Lancaster B, Adams PR, Nicoll, RA (1985) Two distinct Ca-activated K currents in bullfrog sympathetic ganglion cells. Proc Natl Acad Sci USA 82:3040–3044.

Rae J, Cooper K, Gates P, Watsky M (1991) Low access resistance perforated patch recordings using amphotericin-B. J Neurosci Methods 37:15–26.

Reinhart PH, Chung S, Levitan IB (1989) A family of calcium-dependent potassium channels from brain. Neuron 2:1031–1041.

Role LW, Perlman, RL (1980) Purification of adrenal medullary chromaffin cells by density gradient centrifugation. J Neurosci Methods 2:253–265.

Saito M, Nelson C, McCobb D, Salkoff L, Lingle CJ (1994) Molecular analysis of BK channels in adrenal chromaffin and PC12 cells. Soc Neurosci Abstr 20:722.

Solaro CR, Lingle CJ (1992) Trypsin-sensitive, rapid inactivation of a calcium-activated potassium channel. Science 257:1694–1698.

Tomlinson A, Durbin J, Coupland RE (1987) A quantitative analysis of rat adrenal chromaffin tissue: morphometric analysis at tissue and

cellular levels correlated with catecholamine content. Neuroscience 20:895–904.

Verhofstad AAJ, Coupland RE, Parker TR, Goldstein M (1985) Immunohistochemical and biochemical study on the development of the noradrenaline- and adrenaline-storing cells of the adrenal medulla of the rat. Cell Tissue Res 242:233–243.

Vollmer RR, Baruchin A, Kolibal-Pegher SS, Corey SP, Stricker EM, Kaplan BB (1992) Selective activation of norepinephrine- and epinephrine-secreting chromaffin cells in rat adrenal medulla. Am J Physiol 263:R716–721.

Yellen G (1984) Ionic permeation and blockade in Ca^{2+}-activated K^+ channels of bovine chromaffin cells. J Gen Physiol 84:157–186.